Journal of Chemical&Engineering Data

pubs.acs.org/jced

Article

Thermodynamic Characterization of Gas Mixtures for Non-Thermal Plasma CO_2 Conversion Applications with Soft-SAFT

Cristina Mas-Peiro, Héctor Quinteros-Lama, Josep Oriol Pou, and Fèlix Llovell*

Cite This: *J. Chem. Eng. Data* 2023, 68, 1376−1387

Read Online

ACCESS | Metrics & More | Article Recommendations | Supporting Information

ABSTRACT: Carbon dioxide (CO_2) transformation into added-value products through non-thermal plasma (NTP) represents a novel technology of interest. The process involves, apart from CO_2, mixtures of different gases such as carbon monoxide (CO), oxygen (O_2), nitrogen (N_2), argon (Ar), and hydrogen (H_2) for subsequent CO_2 methanation. In this work, a preliminary study of the thermodynamic representation of the mixtures relevant in the context of carbon capture, utilization, and storage (CCUS) processes, but focused on the NTP conversion, is presented. The thermodynamic characterization is achieved through the application of the polar soft-statistical associating fluid theory (SAFT) equation of state (EoS), which allows molecular parameterization of pure compounds and the description of mixtures at different conditions of temperature and pressure. An accurate parametrization of all gases is carried out by explicitly considering the quadrupolar nature of CO_2, CO, and N_2. The characterization is then used to describe several single-phase densities, derivative properties, second virial coefficients, and the vapor−liquid equilibrium (VLE) of CO_2 binary mixtures with Ar, O_2, CO, N_2, and H_2, as well as combinations between some of these gases. A parametric analysis of the impact of the binary parameters on the equilibria description is carried out to assess the temperature dependency. The results have overall shown good agreement to experimental data in most conditions using one or two binary parameters. Finally, ternary systems involving CO_2, O_2, Ar, and N_2 have been predicted in good agreement with the experimental data, demonstrating the capacity of the model to evaluate the behavior of multicomponent gas mixtures.

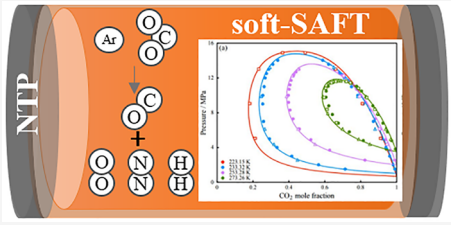

1. INTRODUCTION

The increasing amount of anthropogenic CO_2 emissions has been a major contributor to global warming. According to the very recent 6th Assessment IPCC Report, evidence suggests that around 64% of GHG emissions come from CO_2 originated from fossil fuels and industrial processes.[1] As a consequence, limiting these CO_2 emissions becomes imperative. In this regard, carbon capture, utilization, and storage (CCUS) methods play an important role in net-zero energy systems as they contribute to both reducing and utilizing CO_2 emissions.[2] In fact, CCUS involves a diverse variety of techniques, developments, and potential applications of high interest. The reader is referred to the recent detailed review of Zhu for further details.[3] In particular, CO_2 usage technologies introduce opportunities to partially substitute fossil-fuel raw materials to increase the use of renewable energy as alternatives, as well as to generate income by producing marketable fuel products.

CO_2 usage can be understood as either a direct utilization or a conversion to other chemicals and energy products. On one side, in direct utilization, CO_2 is used as a commercial product in the food and beverage industry or as a solvent in supercritical extraction of natural products, among other industrial applications.[4] On the other side, CO_2 conversion involves the use of CO_2 as a reactant to be converted into other chemicals or energy products, either through carboxylation reactions in which CO_2 is used to obtain organic compounds (including carbonates, acrylates, and polymers) or through reduction reactions where the C═O bonds are broken to produce other chemicals (including methane, methanol, urea, syngas, and formic acid).[5,6] The limitation of CO_2 conversion is the energy intensive nature of these processes due to the high thermodynamic stability of the CO_2 molecule.[7]

CO_2 conversion methods are frequently grouped into: hydrogenation,[8] electro-catalytic/electrochemical reduction,[5] enzymatic/biochemical processes,[5] photo-reduction,[5,9,10] or plasma processes, such as non-thermal plasma (NTP).[3,11−14] The resulting products generated in each of these processes are varied but primarily include: hydrocarbons, hydrogen, and oxygenates via catalytic conversion; and carbon monoxide, hydrocarbons, syngas, and oxygenates from plasma processes.[7,14] These products have the potential to replace petrochemical feedstocks as the process results in added-value chemicals and fuels.[15]

Received: February 27, 2023
Accepted: April 14, 2023
Published: May 16, 2023

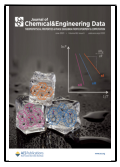

Downloaded from pubs.acs.org/jceaax/article-pdf/68/6/1376/9199119/je3c00131.pdf by guest on 30 September 2026

ACS Publications

© 2023 The Authors. Published by American Chemical Society

Among these many CO_2 utilization technologies, a conversion method of growing interest is NTP reduction.[11−14,16] NTP is generated by applying a potential difference between two electrodes, which are inserted in a reactor filled with gas.[16] When electrons are accelerated by the electric field generated, they collide toward gas molecules, resulting in ionization, excitation, and dissociation. The dissociation collisions create radicals with enough energy input to break the OC═O double bond at atmospheric conditions. It is under this principle that gas conversion applications occur. This technology can be operated at ambient temperature while still generating highly active species and electrons, representing a low energy process compared to conventional thermal plasma conversion.

The problem of gas mixtures has been addressed in the past for CO_2 transport, focusing on the presence of small impurities and their influence in the thermophysical behavior of the CO_2 stream for pipeline design. In this work, the focus intends to expand the understanding of CCUS to assess the thermophysical behavior of gas mixtures involved in CO_2 decomposition through NTP in a fluidized plasma reactor (FPR). The electrons produced in the plasma acquire high energies (between 1 and 10 eV), and research shows that the use of argon (Ar) as a diluent gas proves beneficial in CO_2 conversion[17] due to the lower minimum voltage required to form plasma with Ar. In effect, NTP decomposes CO_2 into carbon monoxide (CO) and oxygen (O_2) with the use of Ar as a diluent gas.[17] Alternatively, other studies have shown the possibility to perform the process in a nitrogen (N_2) environment, resulting in an overall lower cost.[18] Subsequently, the CO produced is usually coupled with a hydrogen source (H_2) to produce syngas (CH_4).[19] In summary, mixtures of CO_2 with Ar, CO, O_2, N_2, H_2, and CH_4 can be found in NTP processes in a wide variety of compositions.

In this context, although extensive work has been devoted to the thermodynamic characterization of CO_2 mixtures, a review of the literature still identifies several gaps of knowledge, particularly when addressing either properties different than vapor−liquid equilibria (VLE) (i.e. second-order derivative properties) or when describing the behavior of multicomponent mixtures. From a modeling perspective, the use of equations of state (EoSs), ranging from empirically specific-compound equations, classical and/or refined cubic equations, and statistical-mechanics-based equations, is common in the description of CO_2 mixtures in CCUS processes.

While it is not possible to review all works done in the area (the reader is referred to the extensive review of Li and coworkers[20] for further details), it is important to highlight some notable approaches. Among the semi-empirical EoSs developed for combustion gases, named EoS-CG, the equation of Span and Gernert,[21] derived from the Span and Wagner EoS for pure CO_2,[22] provides very high accuracy for the single and phase equilibria of mixtures with CO_2, CO, N_2, H_2, Ar, and H_2O at wide-ranging conditions. However, as any empirically-fitted equation, it suffers limitations when generalized to other components or conditions. Another pressure-explicit EoS studying these CCUS mixtures that has shown favorable results is the one published by Demetriades and Graham.[23] In terms of cubic equations, Peng−Robinson (PR) has been extensively used for these systems, completing experimental measurements, such as in the work of Vega-Maza and coworkers,[24] who provided new experimental data on the CO_2−H_2 and CO_2−N_2 mixtures, modeling them with PR. The work of Carroll[25] also includes the PR equation, as well as the Soave−Redlich−Kwong (SRK) EoS, to study CO_2 mixtures with H_2S and CH_4. In addition, several authors provide a comparison between molecular-based statistical associating fluid theory (SAFT) equations and empirical or cubic thermodynamic models, as is the case for by Diamantonis et al.,[26] whose work provides a comparison between the SAFT,[27,28] PC-SAFT,[29] and EoS-CG models for CO_2-rich multicomponent mixtures. Other SAFT models relevant in the context of CCUS (SAFT-VR Mie,[30] based on the Mie intermolecular potential) are also compared in another contribution.[31]

In this work, the polar version of soft-SAFT,[32] an adequate thermodynamic model to treat the polarity in gases, is used to characterize the thermodynamic behavior of mixtures involved in CO_2 conversion processes with particular focus on the description of binary and ternary mixtures of common CCUS compounds relevant to NTP conversion: carbon dioxide (CO_2), argon (Ar), oxygen (O_2), carbon monoxide (CO), hydrogen (H_2), and nitrogen (N_2). Previous work shows that soft-SAFT has been successfully used to determine thermodynamic properties and phase equilibria calculations for other CO_2 mixtures involving a wide variety of compounds and solvents, such as polyether blends,[33] perfluoroalkanes,[34] monoethalonamine (MEA),[35] aqueous and non-aqueous amine hybrid solvents,[36,37] ionic liquids,[38] and deep eutectic solvents,[39] as well as CH_4.[40]

The present contribution is organized as follows: an initial overview of the theoretical background on soft-SAFT EoS is provided. Then, results for CCUS relevant compounds are presented and discussed: density behavior, derivative properties, second virial coefficients and VLE of CO_2 binary mixtures, thermodynamic VLE of other non-CO_2 binary mixtures, and, finally, the characterization of two ternary mixtures: CO_2, O_2, and Ar and CO_2, O_2, and N_2. Lastly, some concluding remarks are provided on the applicability of the soft-SAFT EoS in the context of CCUS.

2. THEORETICAL BACKGROUND AND METHODOLOGY

2.1. Soft-SAFT. Soft-SAFT[41,42] is a well-known, mature variant of the original SAFT,[27,28] a molecular-based EoS developed from statistical mechanics concepts that is capable of describing thermodynamic properties of complex fluids. It is obtained from Wertheim's first-order thermodynamic perturbation theory (TPT1) and accounts for different microscopic contributions such as high-range directional forces and chain formation.[43−46]

As any SAFT model, soft-SAFT is expressed as the addition of residual Helmholtz energy of the system accounting for different microscopic contributions representing different molecular effects. For the particular case of non-associating ($A^{assoc} = 0$) polar molecules, such as those treated in this work, the equation reads:

$$A^{res} = A^{ref} + A^{chain} + A^{polar} \quad (1)$$

where A^{res} is the residual Helmholtz free energy ($A^{total} - A^{ideal}$), A^{ref} accounts for the free energy of reference of the component (understood as interaction between monomers), A^{chain} is the contribution due to chain formation, and A^{polar} accounts for component polarity. The reference term in soft-SAFT, A^{ref}, employs the Lennard−Jones (LJ) intermolecular potential for the repulsive and attractive interactions, computed following

https://doi.org/10.1021/acs.jced.3c00131
J. Chem. Eng. Data 2023, 68, 1376−1387

Downloaded from pubs.acs.org/jceaax/article-pdf/68/6/1376/9199119/je3c00131.pdf by guest on 30 September 2026

the work of Johnson et al.[47] The expressions of the chain term, A^{chain}, resulting from Wertheim's theory (TPT1), is similar to other SAFT EoS versions. The contribution of multipolar interactions, A^{polar}, is obtained from the approach proposed by Gubbins and Twu,[48,49] initially developed for spherical molecules and later extended to chains by Jog et al.[50] The perturbative theory used to develop the polar expression explicitly includes the polar moment (either the dipole, μ, or the quadrupole, Q), as well as another parameter representing the fraction of polar segments in a molecule (x_p). In this work, we are employing the interpolation equations for the integrals over pair and triplet correlation functions of a LJ fluid drawn from the work of Luckas et al.[51] The reader is referred to the original soft-SAFT articles, including the subsequent addition of the polar contribution, for further details.[32,41,42]

Based on the different terms previously shown, the description of the gases studied here within the soft-SAFT framework is given through a coarse-grained model defined by a homonuclear chain of m spherical segments of diameter σ_{ii} and dispersive energy between segments (ε_{ii}). In the case of quadrupolar fluids, the set of molecular parameters is completed with the effective quadrupolar moment (Q) and the fraction of segments containing the polar moment (x_p). This set of molecular parameters is sufficient to characterize a fluid and is usually obtained by fitting to experimental equilibrium data, most notably liquid density and vapor pressure data in a range of temperatures (from triple point, T_{tp}, to 0.95 times the critical temperature, T_c).

The extension of the theory to mixtures is straightforward for the case of the chain and polar terms as they are explicitly defined for mixtures. Concerning the reference LJ term, the segment diameter and different dispersive energies have to be averaged by generating a pseudo-compound with the thermodynamic properties of the mixture. This computational extension is achieved through the van der Waals one-fluid theory with the generalized Lorentz−Berthelot (LB) combining rules:

$$\sigma_{ij} = \eta_{ij}\left(\frac{\sigma_{ii} + \sigma_{jj}}{2}\right) \tag{2}$$

$$\varepsilon_{ij} = \xi_{ij}\sqrt{\varepsilon_{ii}\,\varepsilon_{jj}} \tag{3}$$

where σ_{ij} and ε_{ij} are the crossed segment diameter and dispersive energy for the mixture, and η_{ij} and ξ_{ij} are the adjustable size and energy binary parameters to account for deviations from the LB rule. These parameters consider the differences in size and/or energy between the monomers from the compounds in the mixture, and they are commonly fitted to isothermal or isobar equilibrium data.

2.2. Molecular Models. In this work, six gases have been modeled: CO_2, CO, N_2, O_2, H_2, and Ar as indicated in Table 1.

Table 1. Chemical Compounds and Models

chemical name	chemical formula	CAS number	model
carbon dioxide	CO_2	124-38-9	soft-SAFT
carbon monoxide	CO	630-08-0	soft-SAFT
nitrogen	N_2	7727-37-9	soft-SAFT
oxygen	O_2	7782-44-7	soft-SAFT
hydrogen	H_2	1333-74-0	soft-SAFT
argon	Ar	7440-37-1	soft-SAFT

All are described as homonuclear chains of m spherical segments of diameter σ and monomer−monomer dispersive energy ε/k_B. The quadrupole effect in CO_2, CO, and N_2 has been explicitly considered. In this case, the polarity fraction is fixed a priori, and the quadrupole moments are obtained from experimental values.[36] As in previous studies,[52,53] dipole moment of CO is not taken into account in the molecular characterization due to its very low value (μ = 0.122 Debye).[54] In the case of O_2 and H_2, their very low polarity is considered negligible for their characterization and no quadrupole moment is explicitly expressed. Concerning Ar, an apolar spherical molecule, an additional constraint is imposed by fixing the chain length (m) to 1. The final set of optimized molecular parameters for all compounds is taken from previous contributions, with the exception of Ar, which has been refitted using saturated liquid density and vapor pressure data to improve its phase equilibrium description. Table 2 summarizes the molecular parameters of all the compounds involved in this work.

The phase equilibrium of the thermodynamic behavior of Ar is presented in Figure S1 of the Supporting Information. Excellent agreement is found between the experimental data and the soft-SAFT description with an average absolute deviation (AAD%) of 0.717 and 1.076% for the saturated liquid density and vapor pressure, respectively.

3. RESULTS AND DISCUSSION

3.1. Binary Mixtures Characterization. Once the parameters for the pure gases are well established, binary mixtures are characterized. The CO_2 binary mixtures modeled in the present work are mixtures of CO_2 with Ar, O_2, CO, N_2, and H_2. Additional binary mixtures without CO_2 include O_2 and Ar, CO and N_2, and CO and Ar. A summary of all calculations carried out for all mixtures, including all properties and operating conditions (temperature, pressure, and composition) are summarized in Table S1 in the Supporting Information.

First, the single-phase density of several CO_2 mixtures is predicted at different temperatures, ranging from the subcritical till the supercritical region, as shown in Figures 1 and S3a (for CO_2−H_2) in the Supporting Information.

The comparison with experimental data reveals very good agreement for all the mixtures studied with some minor deterioration at the highest pressures and lowest temperatures for the CO_2−Ar system. The information provided by the equation is useful given the experimental gaps noticed for several mixtures. In particular, $p\rho T$ experimental data are scarce for the CO_2−CO mixture,[58] of particular interest in this work, as it only covers a small phase region.

Apart from the effect of the pressure on the density, it is desirable to analyze additional properties to check the validity of the parametrization. The use of derivative properties is always a good test as they are more sensitive to deviations than primary properties. In Figure 2, the speed of sound at different isotherms is predicted as a function of pressure for the CO_2−Ar mixture at two given compositions. The speed of sound can be estimated from the combination of other derivative properties, such as the isochoric and isobaric heat capacities, according to:

$$\omega = \sqrt{\frac{C_p}{C_v}\left(\frac{1}{\rho \times k_T}\right)} \tag{4}$$

https://doi.org/10.1021/acs.jced.3c00131
J. Chem. Eng. Data 2023, 68, 1376−1387

Downloaded from pubs.acs.org/jceaax/article-pdf/68/6/1376/9199119/je3c00131.pdf by guest on 30 September 2026

Table 2. Optimized Soft-SAFT Molecular Parameters for All Pure Compounds

compound	m	σ (Å)	ε/k_B (K)	$Q \times 10^{40}$ ($C \times m^2$)	x_P	reference
CO_2	1.571	3.166	166.5	14.68	0.333	40
CO	1.156	3.500	85.5	9.473	0.500	40
N_2	1.304	3.291	85.2	4.53	0.500	40
O_2	1.168	3.198	111.5			55
H_2	0.487	4.244	33.9			55
Ar	1.000	3.401	117.1			this work

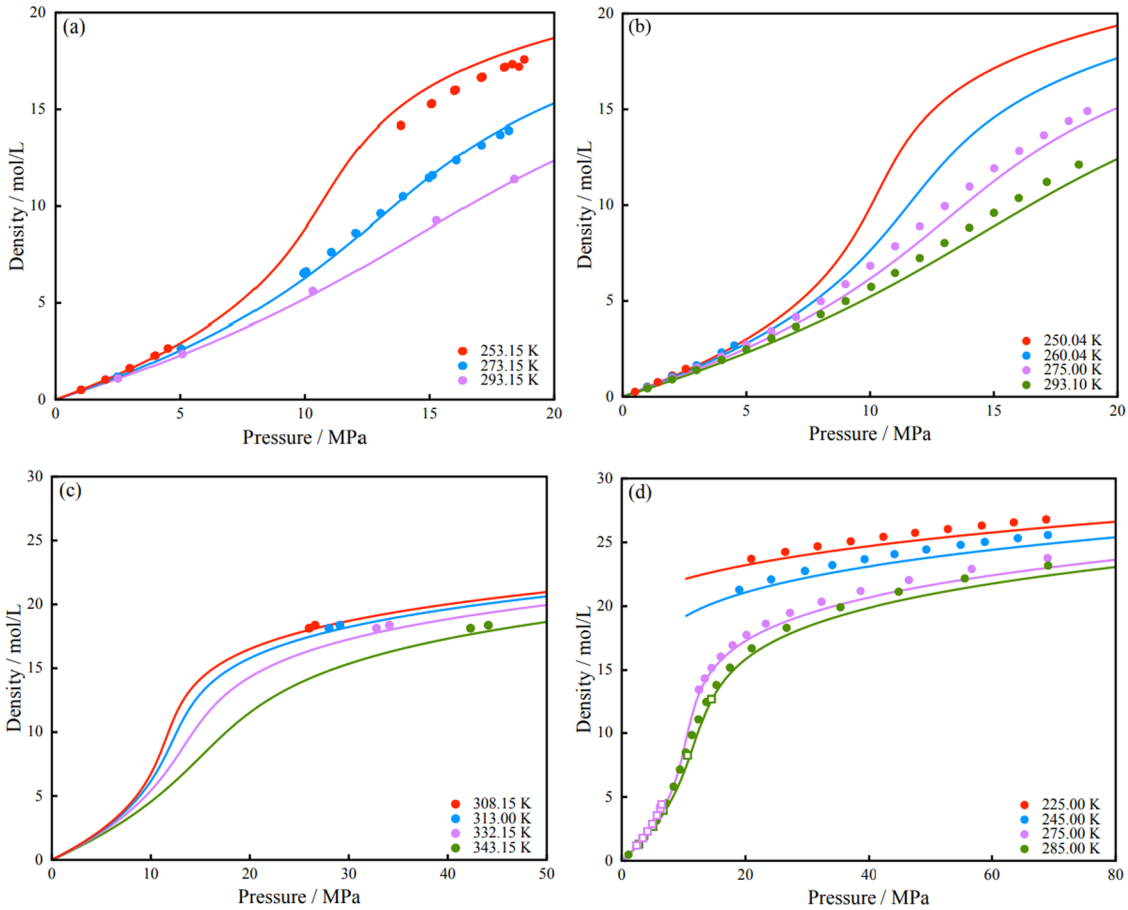

Figure 1. Isothermal density−pressure diagrams of CO_2 mixtures with (a) 50% Ar with experimental data (circles[56]), (b) 50% O_2 with experimental data (circles[57]), (c) 13.8% CO with experimental data (circles[58]), and (d) 28.895% N_2 with experimental data (squares[59] and circles[60]). In all cases, soft-SAFT calculations are represented by full lines.

where c_p and c_v are the isobaric and isochoric heat capacities, respectively, k_T is the reduced bulk modulus, and ω is the speed of sound. In these calculations, the ideal contribution to the heat capacities is added from the available correlations given at NIST.[61] Good agreement is found in all cases, with a very slight over prediction at the lowest temperatures. Still, the qualitative prediction is excellent, given the sensitivity of this property.

Given the fact that the speed of sound has been compared at isotherms which are at a temperature higher than the working conditions of interest, other properties have been evaluated so as to further validate the approach. In Figure 3a, the isothermal compressibility as a function of pressure of the CO_2−Ar mixture has been predicted in a wide range of temperatures. In this system, the predictions underestimate the isothermal compressibility values although good qualitative behavior is achieved in all cases.

In addition, the prediction of the second virial coefficient for the same mixture (CO_2−Ar), which is a reliable assessment to check the validity of the model, has been included. Notice that the green line represents pure argon, showing an excellent agreement with the data. The second virial coefficient of the mixtures is also in good agreement with the experimental data with some minor deviations that are constant in the whole temperature range of study (250−350 K).

Next step concerns the evaluation of the binary VLE of these systems. The study of the VLE of CO_2-gas mixtures has already been described by other SAFT-type equations as mentioned in the literature.[26,31,65] The nature of these mixtures does not allow quantitative agreement without further adjustment of binary parameters, a common characteristic in all previous bibliography efforts. When using soft-SAFT, a similar performance was found (prediction using combining rules without any binary parameter deviates from the experimental data as shown in Figure S2 of the Supporting Information for the mixture

https://doi.org/10.1021/acs.jced.3c00131
J. Chem. Eng. Data 2023, 68, 1376−1387

Downloaded from pubs.acs.org/jceaax/article-pdf/68/6/1376/9199119/je3c00131.pdf by guest on 30 September 2026

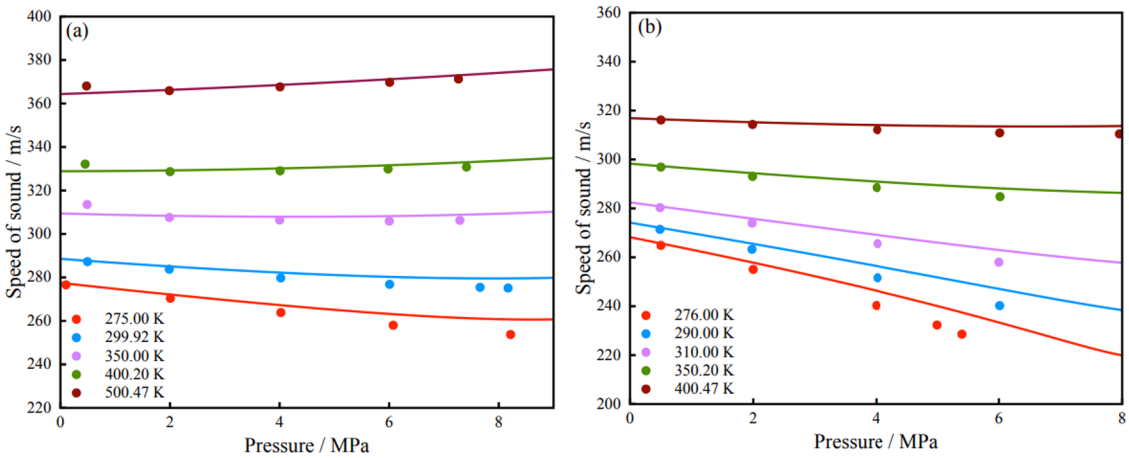

Figure 2. Isothermal speed of sound−pressure diagrams for CO_2 and Ar mixture with CO_2 compositions of (a) x_{CO2} = 0.50104 and (b) x_{CO2} = 0.74981. In all cases, symbols[56] are experimental data and full lines represent soft-SAFT predictions.

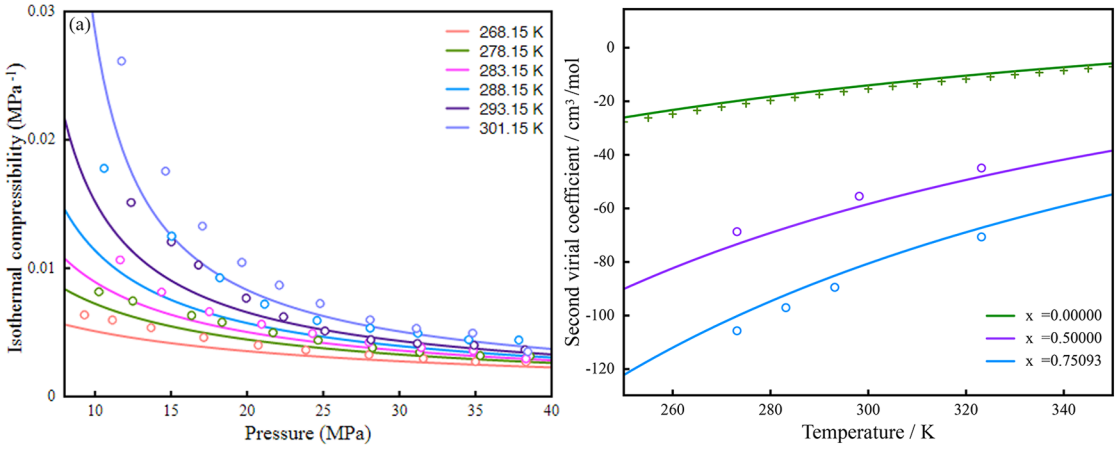

Figure 3. Predicted properties for the CO_2 + Ar mixture. (a) Isothermal Compressibility of CO_2 with Ar at x_{CO2} = 0.0446 and different temperatures. Symbols represent experimental data.[64] (b) Second virial coefficients of pure Ar and a mixture of CO_2 (1) with Ar (2) as a function of temperature at different compositions. Crosses,[62] and circles,[63] represent experimental data. In both Figures, lines are the soft-SAFT predictions.

CO_2−Ar). This is a consequence of the incondensable nature of the gases involved and the arbitrary choice of the combining rules. Consequently, and following the same procedure done by other authors,[26,31,65] a correcting size and energy binary parameters (η and ξ, respectively) are introduced to fit the results at all isotherms using available experimental data. In this work, the VLE representation of all the mixtures is achieved with a constant binary energy parameter (ξ) close to unity, while a binary temperature-dependent size parameter η has been fitted and correlated with a second-order polynomial form for the CO_2-gas mixtures. The only exception is the CO_2−H_2 mixture, where a good description for all mixtures is achieved without using any size parameter.

Although it seems more common to establish an energy temperature-dependent binary parameter, we have noticed that a size binary parameter can better capture the VLE behavior of gas mixtures due to entropic effects as a consequence of the relatively low energy interaction with incondensable gases such as Ar, N_2, CO, or H_2. In order to demonstrate this sensitivity of the η binary parameter on the VLE description, a complete characterization study of the impact of both binary parameters, η and ξ, has been carried out using the CO_2−Ar system at the benchmark system. Figure 4 shows a parametric analysis of the carbon dioxide plus argon system at four temperatures. The average deviation (%) contrasted with the experimental data is displayed as contour plots.

In Figure 4, each projection shows summit and valley areas, particularly at low temperatures, caused by the emergence of equilibrium features, such as liquid−liquid equilibrium (see Figure 4a). In all cases, the global minimum is highlighted with (A) for each temperature and lies in a coordinate where both interaction coefficients are different than one. Points (X) are the interaction parameters selected in the study using the presented correlation. In two cases, Figure 4b,d, point (A) matches with point (X). Additionally, at all temperatures, the ADD of points (A) and (X) are <1.60% and <3.00%, respectively. Other valley zones appear as in Figure 4b, highlighted in point (B). These local optima are discarded due to the underprediction of the mixture critical point.

The most relevant conclusion of the study is the fact that while the ξ dispersive interaction coefficient has a stable value of around 1.01 in all cases, the η optimum is more affected by the temperature change. More importantly, it can be seen that the blue areas (indicating the lowest deviations) cannot be achieved using an η parameter equal to unity. Indeed, the η parameter becomes significantly higher than 1 at the highest temperatures. For this reason, a temperature functionality in the η parameter has been used.

https://doi.org/10.1021/acs.jced.3c00131
J. Chem. Eng. Data 2023, 68, 1376−1387

Downloaded from pubs.acs.org/jceaax/article-pdf/68/6/1376/9199119/je3c00131.pdf by guest on 30 September 2026

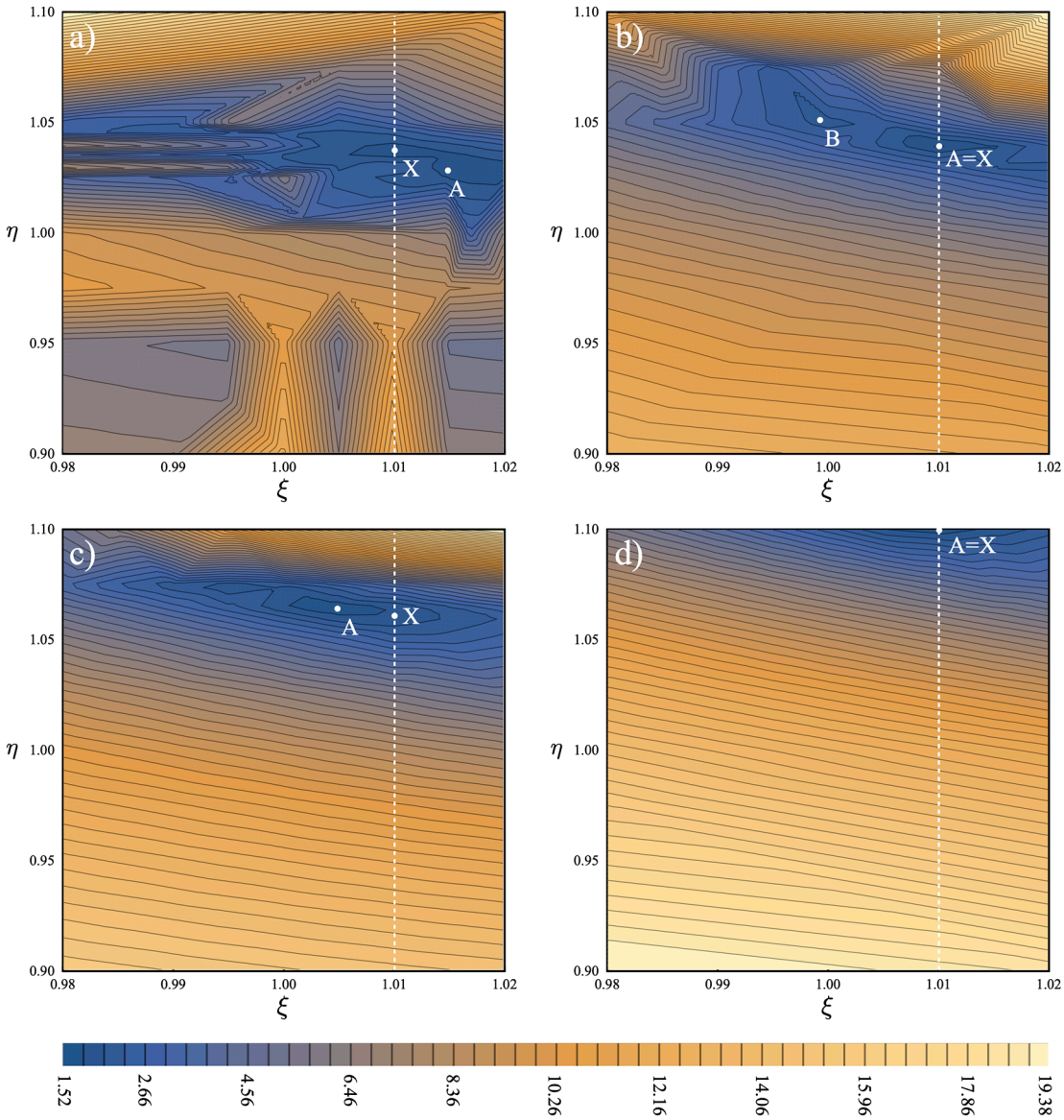

Figure 4. Parametric analysis of the influence of binary parameters ξ and η in the description of the vapor−liquid equilibria of CO_2 with Ar at (a) 223.15 K, (b) 233.32 K, (c) 253.28 K, and (d) 273.26 K. Letter A indicates the minimum absolute average deviation (%AAD), letter B shows a local minimum, and letter X indicates the binary parameter value selected.

A summary of the required coefficients and values for the η and ξ binary parameters, respectively, is given in Table 3. The study of η correlation to temperature allows the extrapolation to other temperatures when lacking experimental data. Still, it is significant to note that limitations on the usage of these correlations can appear when approaching critical boundaries of the mixtures.

Table 3. Summary of Size (η) and Energy (ξ) Binary Parameters[a]

	η			
mixture	$a \times 10^5$	$b \times 10^3$	c	ξ
CO_2−Ar	2.06206	−8.86548	1.98277	1.010
CO_2−O_2	1.12766	−4.45338	1.45999	1.010
CO_2−CO	1.00000	−4.16299	1.47101	1.130
CO_2−N_2	1.58793	−6.96290	1.79146	1.100
CO_2−H_2	0	0	1.00000	1.350

[a] η follows a second-order degree polynomial with temperature according to the expression: $aT^2 + bT + c$.

The final results of the VLE modeling are displayed in Figures 5 and S3b, (for the CO_2−H_2 mixture) in Supporting Information, showing several isotherms for all mixtures (ranging from 218.15 to 293.15 K). As it can be noticed, very good agreement is achieved between the soft-SAFT model (lines) and the available experimental data (symbols). Although some minor discrepancies are observed in the vicinity of the critical point, particularly over ambient temperature (T > 273.15 K), the overall representation provides a reliable characterization of the VLE behavior (Figure 5).

The comparative analysis among the different CO_2-gas mixtures allows better understanding on how they thermodynamically behave. For this purpose, the comparison of five mixtures (including CO_2−H_2) at the same isotherm is

https://doi.org/10.1021/acs.jced.3c00131
J. Chem. Eng. Data 2023, 68, 1376−1387

Downloaded from pubs.acs.org/jceaax/article-pdf/68/6/1376/9199119/je3c00131.pdf by guest on 30 September 2026

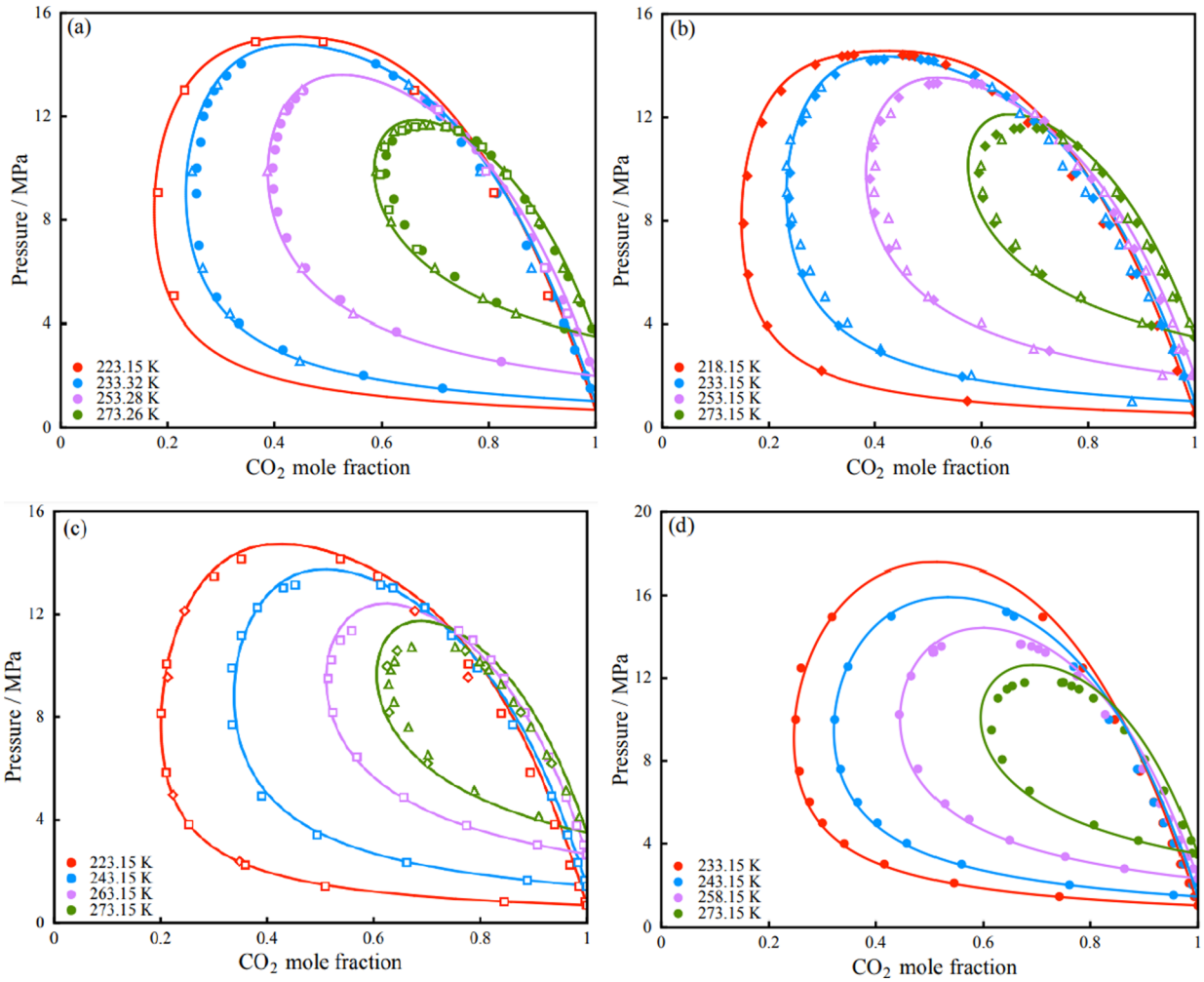

Figure 5. Isothermal vapor−liquid equilibrium of CO_2 at four temperatures with (a) Ar with experimental data (filled circles,[66] squares,[67] and triangles[68]), (b) O_2 with experimental data (triangles[69] and filled diamonds[70]), (c) CO with experimental data (squares,[71] diamonds,[68] and triangles[72]), and (d) N_2 with experimental data (circles[24]). In all cases, soft-SAFT calculations are represented by full lines.

presented in Figure 6. While several mixtures behave similarly at higher concentrations of CO_2 in the vapor phase, remarkable variations are observed in the liquid phase and, consequently, in the phase envelope. While the effect of Ar, O_2, and CO is very similar, the addition of nitrogen notably increases the vapor pressure of the system. Finally, the impact of H_2 is dramatic due to the presence of small hydrogen molecules in the system. It is interesting to note that these differences can be observed in the values of the soft-SAFT molecular parameters included in Table 2.

In this work, other prevalent binary mixtures not containing CO_2 have also been characterized with the soft-SAFT EoS, considering they can be found in NTP conversion processes. A major limitation in these non-CO_2 mixtures is the limited availability of VLE data, particularly in the case of binary mixtures with carbon monoxide as it occurs for the CO−O_2 and CO−H_2 mixtures, where no experimental data have been found. This data scarcity is possibly due to the difficulty in working at very low temperatures as a consequence of the low critical points of these gases.

The description of the O_2−Ar and CO−N_2 mixture in the range 68−100 K is given in Figure 7. It is notable to remark that the absence of CO_2 increases the ideality of the system and, consequently, excellent agreement can be found using a

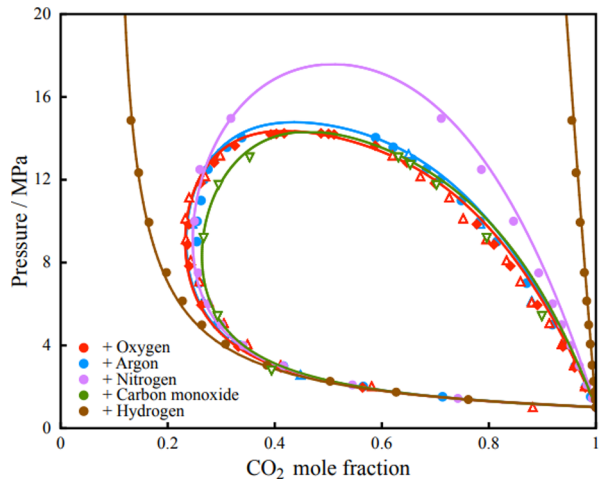

Figure 6. Isothermal vapor−liquid equilibrium of CO_2 mixtures at 233 K with Ar (experimental data: circles[73]), O_2 (experimental data: triangles[69] and diamonds[70]), CO (experimental data: inverted triangles[71]), N_2 (experimental data: circles[24]), and H_2 (experimental data: circles[74]). Soft-SAFT calculations are represented by full lines.

single ξ binary parameter (while η is set to unity), which also turns out to be very close to 1.00 in most cases (O_2 and Ar: ξ =

https://doi.org/10.1021/acs.jced.3c00131
J. Chem. Eng. Data 2023, 68, 1376−1387

Downloaded from pubs.acs.org/jceaax/article-pdf/68/6/1376/9199119/je3c00131.pdf by guest on 30 September 2026

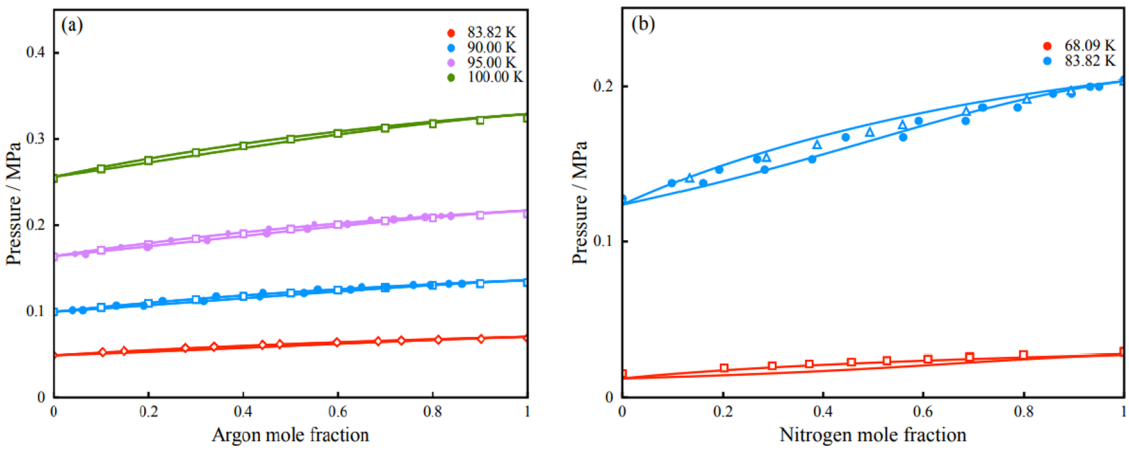

Figure 7. Isothermal vapor−liquid equilibrium of (a) O_2 and Ar mixture with experimental data (squares,[75] filled circles,[76] and diamonds[77]), and (b) CO and N_2 with experimental data (triangles,[77] filled circles,[78] and squares[79]). In all cases, soft-SAFT calculations are represented by full lines.

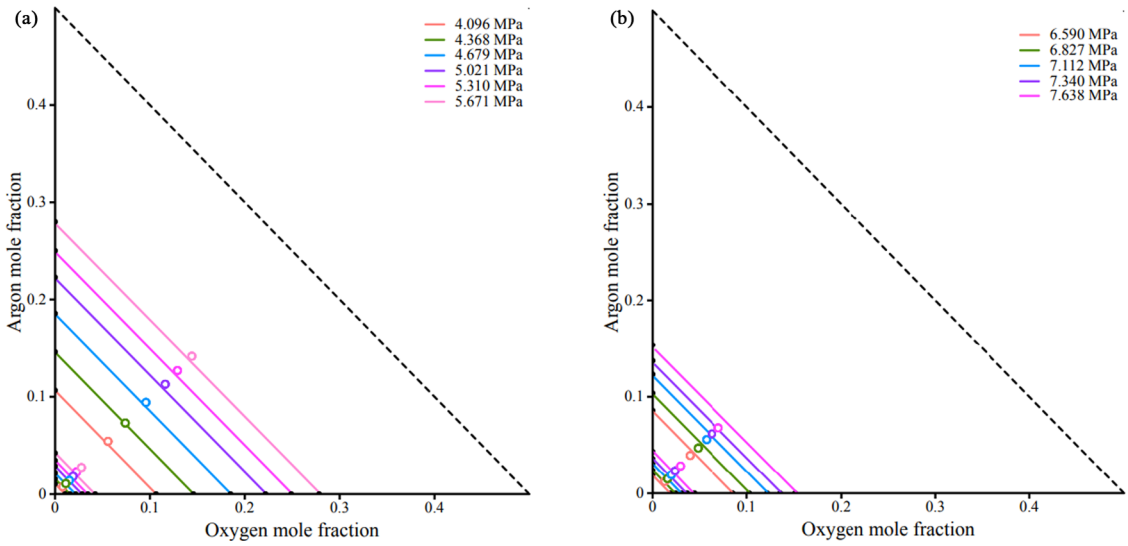

Figure 8. Ternary diagram of CO_2, O_2, and Ar mixture at (a) T = 273.24 K and (b) T = 293.21 K. In all cases, symbols are experimental data (circles[73]) and soft-SAFT predictions are represented by full lines.

0.99, CO and N_2: ξ = 1.01). Additionally, the mixture of CO−Ar (ξ = 1.06), also with η set to unity, can be found in Figure S4 in the Supporting Information.

3.2. Ternary Mixture. One of the main goals of this characterization is to be capable to reproduce multicomponent mixtures. Curiously, although the interest for these mixtures is evident and has practical applications, the amount of work devoted to the description and modeling of ternary systems decreases exponentially compared to binary systems. The previous characterization should enable soft-SAFT to estimate ternary data. Considering that CO_2, O_2, and Ar or N_2 (depending on the type of diluent gas used) are the compounds with the highest concentrations in NTP CO_2 conversion processes, ternary mixtures of CO_2, O_2, and one of these inert gases are particularly important for the current study.

First, the ternary equilibrium of this system (CO_2, O_2, and Ar) is predicted at three different temperatures and several isobars, and compared to experimental data sets,[73] as depicted in Figures 8 and S5 (Supporting Information). In all cases, binary parameters are transferred for each binary pair without further adjustment at 273.24 K, while the parameter correlations are used, when necessary, to predict the behavior at 293.21 K. In both cases, soft-SAFT described the vapor−liquid phase boundaries of the system in good agreement with the experimental data with slight deviations in the vapor phase that increase with the pressure. Still, the results are satisfactory, showing the predictive capacity of the equation. As an additional remark, it is interesting to note that the predictions of these systems without any binary parameter, done for comparison in Figure S6 (Supporting Information), deteriorate at the highest temperature in an equivalent manner as it occurs with the binary systems. These deviations are expected to become more significant at higher pressure if no binary interactions are considered.

In order to extend the validation to other ternary systems, we have also studied the ternary mixture involving CO_2−O_2−N_2 as shown in Figure 9. In this case, the predictions are in excellent agreement with the experimental data for the liquid phase at the two studied temperatures, reaching also a good description of the vapor phase. The quasi-linear behavior of the isobars, already observed in Figure 8, is repeated here.

Finally, it is important to remark that the prediction without binary parameters (see Figure S7 in the Supporting

https://doi.org/10.1021/acs.jced.3c00131
J. Chem. Eng. Data 2023, 68, 1376−1387

Downloaded from pubs.acs.org/jceaax/article-pdf/68/6/1376/9199119/je3c00131.pdf by guest on 30 September 2026

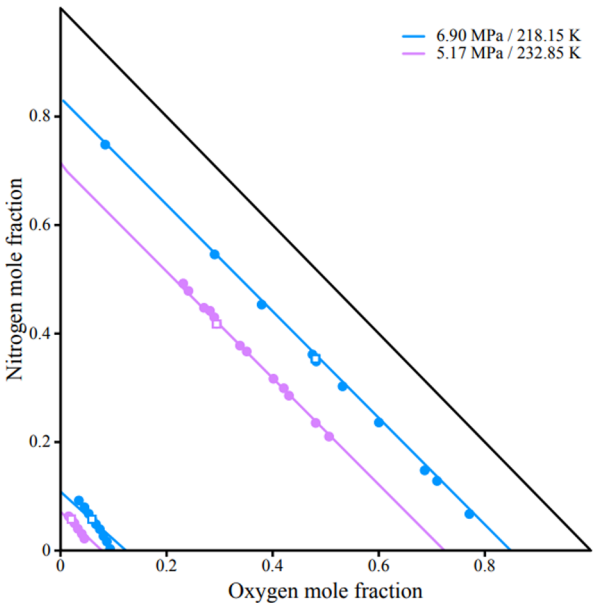

Figure 9. Ternary diagram of CO_2, O_2, and N_2 mixture at T = 218.15 K (blue) and 232.85 K (violet). In all cases, symbols are experimental data (circles[80] and squares[81]) and soft-SAFT predictions are represented by full lines.

Information) reveals severe deviations in the liquid phase. This is the result of an incorrect prediction of the phase behavior of the CO_2−N_2 system without binary parameters, where a Type III behavior is predicted and, consequently, the liquid phase is found at higher pressure. This reinforces the idea that it is necessary to account for the binary interactions so as to ensure a proper description of multicomponent systems.

4. CONCLUSIONS

In this work, the modeling of single-phase and phase equilibria of gas mixtures has been described through soft-SAFT EoS in the context of CO_2 conversion. In particular, a thermodynamic study of the compounds and common impurities involved in NTP CO_2 conversion processes (CO_2, CO, Ar, O_2, N_2, and H_2) has been carried out.

The molecular parameters of all relevant pure substances have been stated from previous literature, except in the case of Ar. These molecular models consider the physical meaning of the molecules, including their polar contributions. In the case of binary mixtures, fitting to experimental data has been achieved through adjustable size and energy binary parameters. A complete parametric analysis has demonstrated the temperature dependency of the size binary parameter exhibited by these gas mixtures. The thermodynamic characterization of each mixture has been completed for a range of conditions with available VLE, including the prediction of $p\rho T$, derivative properties, and second virial coefficients. All mixtures have shown good fitting to experimental data, albeit some limitations appearing when nearing critical regions, as expected. For CO_2-rich mixtures, the correlation found between temperature and binary parameters allows the study of all mixtures in a predictive manner in the case where no experimental data are available at a specific isotherm.

Finally, the study of two ternary mixtures (CO_2 and O_2 with Ar or N_2) has been provided in a fully predictive manner by transferring the binary parameters obtained for the binary systems or using the correlations proposed for these parameters. Results have shown an accurate representation of the multicomponent mixtures' behavior, opening the door for further multicomponent calculations, where data are scarce. These results demonstrate the usefulness of SAFT-type equations, where a balance between complexity and accuracy is achieved.

■ ASSOCIATED CONTENT

Supporting Information

The Supporting Information is available free of charge at https://pubs.acs.org/doi/10.1021/acs.jced.3c00131.

Table S1: Summary of all thermodynamic properties, temperature, pressure, and composition studied in this work; Figure S1: Thermodynamic characterization of argon (Ar) with soft-SAFT; Figure S2: Predicted isothermal vapor−liquid equilibrium of CO_2 with Ar at four temperatures; Figure S3: Isothermal behavior for CO_2 and H_2 mixture at selected temperatures modeled with soft-SAFT (a) density−pressure diagram (b) vapor−liquid equilibrium; Figure S4: Vapor−Liquid equilibrium of CO and Ar mixture modeled with soft-SAFT; Figure S5: Predicted ternary diagram of CO_2, O_2, and Ar mixture at (a) T = 253.27 K; Figure S6: Predicted ternary diagram of CO_2, O_2, and Ar mixture at (a) T = 273.24 K and (b) T = 293.21 K at different isobars with and without transferring binary parameters; Figure S7: Predicted ternary diagram of CO_2, O_2, and N_2 mixture at T = 218.15 K (blue) and 232.85 K (violet) (PDF)

■ AUTHOR INFORMATION

Corresponding Author

Fèlix Llovell − *Department of Chemical Engineering, ETSEQ, Universitat Rovira i Virgili, 43007 Tarragona, Spain;* orcid.org/0000-0001-7109-6810; Email: felix.llovell@urv.cat

Authors

Cristina Mas-Peiro − *Department of Chemical Engineering and Materials Science, IQS School of Engineering, Universitat Ramon Llull, 08017 Barcelona, Spain*

Héctor Quinteros-Lama − *Department of Industrial Engineering, Universidad de Talca, 3341717 Curicó, Chile*

Josep Oriol Pou − *Department of Chemical Engineering and Materials Science, IQS School of Engineering, Universitat Ramon Llull, 08017 Barcelona, Spain;* orcid.org/0000-0003-3179-1688

Complete contact information is available at: https://pubs.acs.org/10.1021/acs.jced.3c00131

Notes

The authors declare no competing financial interest.

■ ACKNOWLEDGMENTS

F.L. and J.O.P. acknowledge financial support from the Spanish Ministry of Science and Innovation MCIN/AEI/10.13039/501100011033/under R + D + I project STOP-F-Gas (Ref: PID2019-108014RB-C21). H.Q.-L. acknowledges funding from FONDECYT, Chile (Project no. 11180103). GESPA (2021 SGR 00321) and AGACAPE (2021 SGR 00738) have been recognized as Consolidated Research Groups by the

https://doi.org/10.1021/acs.jced.3c00131
J. Chem. Eng. Data 2023, 68, 1376−1387

Downloaded from pubs.acs.org/jceaax/article-pdf/68/6/1376/9199119/je3c00131.pdf by guest on 30 September 2026

Catalan Government. Additional funding from 2021 SGR 00738 is also acknowledged.

REFERENCES

(1) Intergovernmental Panel on Climate Change. *IPCC's Sixth Assessment Report*; 2021.

(2) International Energy Agency (IEA). *Special Report on Carbon Capture, Utilisation and Storage: CCUS in Clean Energy Transitions*; 2020.

(3) Zhu, Q. Developments on CO_2-Utilization Technologies. *Clean Energy* **2019**, *3*, 85−100.

(4) Huang, C.-H. H.; Tan, C.-S. S. A Review: CO_2 Utilization. *Aerosol Air Qual. Res.* **2014**, *14*, 480−499.

(5) Yaashikaa, P. R.; Senthil Kumar, P.; Varjani, S. J.; Saravanan, A. A Review on Photochemical, Biochemical and Electrochemical Transformation of CO_2 into Value-Added Products. *J. CO2 Util.* **2019**, *33*, 131−147.

(6) Markewitz, P.; Kuckshinrichs, W.; Leitner, W.; Linssen, J.; Zapp, P.; Bongartz, R.; Schreiber, A.; Müller, T. E. Worldwide Innovations in the Development of Carbon Capture Technologies and the Utilization of CO_2. *Energy Environ. Sci.* **2012**, *5*, 7281−7305.

(7) Cuéllar-Franca, R. M.; Azapagic, A. Carbon Capture, Storage and Utilisation Technologies: A Critical Analysis and Comparison of Their Life Cycle Environmental Impacts. *J. CO2 Util.* **2015**, 82−102.

(8) Saeidi, S.; Amin, N. A. S.; Rahimpour, M. R. Hydrogenation of CO_2 to Value-Added Products—A Review and Potential Future Developments. *J. CO2 Util.* **2014**, *5*, 66−81.

(9) Khan, A. A.; Tahir, M. Recent Advancements in Engineering Approach towards Design of Photo-Reactors for Selective Photo-catalytic CO_2 Reduction to Renewable Fuels. *J. CO2 Util.* **2019**, *29*, 205−239.

(10) Kumar, B.; Llorente, M.; Froehlich, J.; Dang, T.; Sathrum, A.; Kubiak, C. P. Photochemical and Photoelectrochemical Reduction of CO_2. *Annu. Rev. Phys. Chem.* **2012**, *63*, 541−569.

(11) Mei, D.; Tu, X. Conversion of CO_2 in a Cylindrical Dielectric Barrier Discharge Reactor: Effects of Plasma Processing Parameters and Reactor Design. *J. CO2 Util.* **2017**, *19*, 68−78.

(12) Ramakers, M.; Michielsen, I.; Aerts, R.; Meynen, V.; Bogaerts, A. Effect of Argon or Helium on the CO_2 Conversion in a Dielectric Barrier Discharge. *Plasma Processes Polym.* **2015**, *12*, 755−763.

(13) Amouroux, J.; Cavadias, S.; Doubla, A. Carbon Dioxide Reduction by Non-Equilibrium Electrocatalysis Plasma Reactor. *IOP Conf. Ser.: Mater. Sci. Eng.* **2011**, *19*, No. 012005.

(14) Ashford, B.; Tu, X. Non-Thermal Plasma Technology for the Conversion of CO_2. *Curr. Opin. Green Sustainable Chem.* **2017**, *3*, 45−49.

(15) Styring, P.; Jansen, D.; Coninck, H.; Reith, H.; Armstrong, K. *Carbon Capture and Utilisation in the Green Economy. Using CO2 to Manufacture Fuel, Chemicals and Materials*; 2011.

(16) Snoeckx, R.; Bogaerts, A. Plasma Technology-a Novel Solution for CO_2 Conversion? *Chem. Soc. Rev.* **2017**, *46*, 5805−5863.

(17) Pou, J. O.; Colominas, C.; Gonzalez-Olmos, R. CO_2 Reduction Using Non-Thermal Plasma Generated with Photovoltaic Energy in a Fluidized Reactor. *J. CO2 Util.* **2018**, *27*, 528−535.

(18) Ray, D.; Saha, R.; Subrahmanyam, C. DBD Plasma Assisted CO_2 Decomposition: Influence of Diluent Gases. *Catalysts* **2017**, *7*, 244.

(19) Xu, S.; Chansai, S.; Shao, Y.; Xu, S.; Wang, Y.; Haigh, S.; Mu, Y.; Jiao, Y.; Stere, C. E.; Chen, H.; Fan, X.; Hardacre, C. Mechanistic Study of Non-Thermal Plasma Assisted CO_2 Hydrogenation over Ru Supported on MgAl Layered Double Hydroxide. *Appl. Catal., B* **2020**, *268*, No. 118752.

(20) Li, H.; Jakobsen, J. P.; Wilhelmsen, Ø.; Yan, J. PVTxy Properties of CO_2 Mixtures Relevant for CO_2 Capture, Transport and Storage: Review of Available Experimental Data and Theoretical Models. *Appl. Energy* **2011**, *88*, 3567−3579.

(21) Span, R.; Gernert, J.; Jäger, A. Accurate Thermodynamic-Property Models for CO_2-Rich Mixtures. *Energy Procedia* **2013**, *37*, 2914−2922.

(22) Span, R.; Wagner, W. A New Equation of State for Carbon Dioxide Covering the Fluid Region from the Triple-Point Temperature to 1100 K at Pressures up to 800 MPa. *J. Phys. Chem. Ref. Data* **1996**, *25*, 1509−1596.

(23) Demetriades, T. A.; Graham, R. S. A New Equation of State for CCS Pipeline Transport: Calibration of Mixing Rules for Binary Mixtures of CO_2 with N_2, O_2 and H_2. *J. Chem. Thermodyn.* **2016**, *93*, 294−304.

(24) Fandiño, O.; Trusler, J. P. M.; Vega-Maza, D. Phase Behavior of (CO_2 + H_2) and (CO_2 + N_2) at Temperatures between (218.15 and 303.15) K at Pressures up to 15 MPa. *Int. J. Greenhouse Gas Control* **2015**, *36*, 78−92.

(25) Carroll, J. J. Phase Equilibria Relevant to Acid Gas Injection: Part 2 - Aqueous Phase Behaviour. *J. Can. Pet. Technol.* **2002**, *41*, 39−43.

(26) Diamantonis, N. I.; Boulougouris, G. C.; Mansoor, E.; Tsangaris, D. M.; Economou, I. G. Evaluation of Cubic, SAFT, and PC-SAFT Equations of State for the Vapor-Liquid Equilibrium Modeling of CO_2 Mixtures with Other Gases. *Ind. Eng. Chem. Res.* **2013**, *52*, 3933−3942.

(27) Chapman, W. G.; Gubbins, K. E.; Jackson, G.; Radosz, M. SAFT: Equation-of-State Solution Model for Associating Fluids. *Fluid Phase Equilib.* **1989**, *52*, 31−38.

(28) Chapman, W. G.; Gubbins, K. E.; Jackson, G.; Radosz, M. New Reference Equation of State for Associating Liquids. *Ind. Eng. Chem. Res.* **1990**, *29*, 1709−1721.

(29) Gross, J.; Sadowski, G. Perturbed-Chain SAFT: An Equation of State Based on a Perturbation Theory for Chain Molecules. *Ind. Eng. Chem. Res.* **2001**, *40*, 1244−1260.

(30) Lafitte, T.; Apostolakou, A.; Avendaño, C.; Galindo, A.; Adjiman, C. S.; Müller, E. A.; Jackson, G. Accurate Statistical Associating Fluid Theory for Chain Molecules Formed from Mie Segments. *J. Chem. Phys.* **2013**, *139*, 154504.

(31) Perez, A. G.; Coquelet, C.; Paricaud, P.; Chapoy, A. Comparative Study of Vapour-Liquid Equilibrium and Density Modelling of Mixtures Related to Carbon Capture and Storage with the SRK, PR, PC-SAFT and SAFT-VR Mie Equations of State for Industrial Uses. *Fluid Phase Equilib.* **2017**, *440*, 19−35.

(32) Alkhatib, I. I. I.; Pereira, L. M. C.; Torne, J.; Vega, L. F. Polar Soft-SAFT: Theory and Comparison with Molecular Simulations and Experimental Data of Pure Polar Fluids. *Phys. Chem. Chem. Phys.* **2020**, *22*, 13171−13191.

(33) Crespo, E. A.; Amaral, M.; Dariva, C.; Carvalho, P. J.; Coutinho, J. A. P.; Llovell, F.; Pereira, L. M. C.; Vega, L. F. Soft-SAFT Equation of State as a Valuable Tool for the Design of New CO_2 Capture Technologies. In *Abu Dhabi International Petroleum Exhibition & Conference*. Society of Petroleum Engineers: Abu Dhabi, UAE, 2017, p 13, DOI: 10.2118/188464-MS.

(34) Dias, A.; Carrier, H.; Daridon, J.; Pàmies, J.; Vega, L.; Marrucho, I. Vapor-Liquid Equilibrium of Carbon Dioxide-Perfluoroalkane Mixtures: Experimental Data and SAFT Modeling. *Ind. Eng. Chem. Res.* **2006**, *45*, 2341−2350.

(35) Lloret, J. O.; Vega, L. F.; Llovell, F. A Consistent and Transferable Thermodynamic Model to Accurately Describe CO_2 Capture with Monoethanolamine. *J. CO2 Util.* **2017**, *21*, 521−533.

(36) Alkhatib, I. I. I.; Pereira, L. M. C.; Alhajaj, A.; Vega, L. F. Performance of Non-Aqueous Amine Hybrid Solvents Mixtures for CO_2 Capture: A Study Using a Molecular-Based Model. *J. CO2 Util.* **2020**, *35*, 126−144.

(37) Alkhatib, I. I. I.; Pereira, L. M. C.; Vega, L. F. 110th Anniversary: Accurate Modeling of the Simultaneous Absorption of H_2S and CO_2 in Aqueous Amine Solvents. *Ind. Eng. Chem. Res.* **2019**, *58*, 6870−6886.

(38) Llovell, F.; Valente, E.; Vilaseca, O.; Vega, L. F. Modeling Complex Associating Mixtures with [Cn-Mim][Tf2N] Ionic Liquids: Predictions from the Soft-SAFT Equation. *J. Phys. Chem. B* **2011**, *115*, 4387−4398.

(39) Lloret, J. O.; Vega, L. F.; Llovell, F. Accurate Description of Thermophysical Properties of Tetraalkylammonium Chloride Deep

Downloaded from pubs.acs.org/jceaax/article-pdf/68/6/1376/9199119/je3c00131.pdf by guest on 30 September 2026

Eutectic Solvents with the Soft-SAFT Equation of State. *Fluid Phase Equilib.* **2017**, *448*, 81.
(40) Alkhatib, I. I. I.; Llovell, F.; Vega, L. F. Assessing the Effect of Impurities on the Thermophysical Properties of Methane-Based Energy Systems Using Polar Soft-SAFT. *Fluid Phase Equilib.* **2021**, *527*, No. 112841.
(41) Blas, F. J.; Vega, L. F. Prediction of Binary and Ternary Diagrams Using the Statistical Associating Fluid Theory (SAFT) Equation of State. *Ind. Eng. Chem. Res.* **1998**, *37*, 660−674.
(42) Blas, F. J.; Vega, L. F. Thermodynamic Behaviour of Homonuclear and Heteronuclear Lennard-Jones Chains with Association Sites from Simulation and Theory. *Mol. Phys.* **1997**, *92*, 135−150.
(43) Wertheim, M. S. Fluids with Highly Directional Attractive Forces I. Statistical Thermodynamics. *J. Stat. Phys.* **1984**, *35*, 19−34.
(44) Wertheim, M. S. Fluids with Highly Directional Attractive Forces. II Thermodynamic Perturbation Theory and Integral Equations. *J. Stat. Phys.* **1984**, *35*, 35−47.
(45) Wertheim, M. S. Fluids with Highly Directional Attractive Forces III. Multiple Attraction Sites. *J. Stat. Phys.* **1986**, *42*, 459−476.
(46) Wertheim, M. S. Fluids with Highly Directional Attractive Forces IV. Equilibrium Polymerization. *J. Stat. Phys.* **1986**, *42*, 477−492.
(47) Johnson, J. K.; Zollweg, J. A.; Gubbins, K. E. The Lennard-Jones Equation of State Revisited. *Mol. Phys.* **1993**, *78*, 591−618.
(48) Twu, C. H.; Gubbins, K. E. Thermodynamics of Polyatomic Fluid Mixtures—II: Polar, Quadrupolar and Octopolar Molecules. *Chem. Eng. Sci.* **1978**, *33*, 879−887.
(49) Gubbins, K. E.; Twu, C. H. Thermodynamics of Polyatomic Fluid Mixtures—I Theory. *Chem. Eng. Sci.* **1978**, *33*, 863−878.
(50) Jog, P. K.; Sauer, S. G.; Blaesing, J.; Chapman, W. G. Application of Dipolar Chain Theory to the Phase Behavior of Polar Fluids and Mixtures. *Ind. Eng. Chem. Res.* **2001**, *40*, 4641−4648.
(51) Luckas, M.; Lucas, K.; Deiters, U.; Gubbins, K. E. Integrals over Pair- and Triplet-Correlation Functions for the Lennard-Jones (12−6)-Fluid. *Mol. Phys.* **1986**, *57*, 241−253.
(52) Ramos, M.; Docherty, H.; Blas, F.; Galindo, A. Application of the Generalised SAFT-VR Approach for Long-Ranged Square-Well Potentials to Model the Phase Behaviour of Real Fluids. *Fluid Phase Equilib.* **2009**, *276*, 116−126.
(53) Llovell, F.; Vilaseca, O.; Vega, L. F. Thermodynamic Modeling of Imidazolium-Based Ionic Liquids with the [PF 6] - Anion for Separation Purposes. *Sep. Sci. Technol.* **2012**, *47*, 399−410.
(54) Scuseria, G.; Miller, M.; Jensen, F.; Geertsen, J. The Dipole Moment of Carbon Monoxide. *J Chem Phys* **1991**, *94*, 6660−6663.
(55) Pàmies Corominas, J. *Bulk and Interfacial Properties of Chain Fluids: A Molecular Modelling Approach. Ph.D. Thesis.* Universitat Rovira i Virgili, 2004.
(56) Wegge, R. Thermodynamic Properties of the (Argon + Carbon Dioxide) System: Instrument Development and Measurements of Density and Speed of Sound; Ruhr-Universität Bochum, 2016, DOI: 10.13140/RG.2.1.4587.1769.
(57) Lozano-Martín, D.; Vega-Maza, D.; Martín, M. C.; Tuma, D.; Chamorro, C. R. Thermodynamic Characterization of the (CO_2 + O_2) Binary System for the Development of Models for CCS Processes: Accurate Experimental (p, ρ, T) Data and Virial Coefficients. *J. Supercrit. Fluids* **2021**, *169*, No. 105074.
(58) Cipollina, A.; Anselmo, R.; Scialdone, O.; Filardo, G.; Galia, A.; Ed, S. Experimental P - T -G Measurements of Supercritical Mixtures of Carbon Dioxide, Carbon Monoxide, and Hydrogen and Semi-quantitative Estimation of Their Solvent Power Using the Solubility Parameter Concept. *J. Chem. Eng. Data* **2007**, *52*, 2291−2297.
(59) Arai, Y.; Kaminishi, G.-I.; Saito, S. The Experimental Determination of the P-v-t-x Relations for the Carbon Dioxide-Nitrogen and the Carbon Dioxide-Methane Systems. *J. Chem. Eng. Jpn.* **1971**, *4*, 113−122.
(60) Brugge, H. B.; Holste, J. C.; Hall, K. R.; Gammon, B. E.; Marsh, K. N. Densities of Carbon Dioxide + Nitrogen from 225 K to 450 K at Pressures up to 70 MPa. *J. Chem. Eng. Data* **1997**, *42*, 903−907.
(61) IUPAC. *NIST Chemistry WebBook, NIST Standard Reference Database Number 69*; 2007.
(62) *DIPPR 801 Thermophysical Property Database and DIADEM Predictive Software*; 2007.
(63) Souissi, B. M. A.; Kleinrahm, R.; Yang, X.; Richter, M. Vapor-Phase (p, ρ, T, x) Behavior and Virial Coefficients for the Binary Mixture (0.05 Hydrogen + 0.95 Carbon Dioxide) over the Temperature Range from (273.15 to 323.15) K with Pressures up to 6 MPa. *J. Chem. Eng. Data* **2017**, *62*, 2973−2981.
(64) Al-Siyabi, I. *Effect of Impurities on CO2 Stream Properties*; Heriott Watt University, 2013.
(65) Chapoy, A.; Nazeri, M.; Kapateh, M.; Burgass, R.; Coquelet, C.; Tohidi, B. Effect of Impurities on Thermophysical Properties and Phase Behaviour of a CO_2-Rich System in CCS. *Int. J. Greenhouse Gas Control* **2013**, *19*, 92−100.
(66) Coquelet, C.; Valtz, A.; Dieu, F.; Richon, D.; Arpentinier, P.; Lockwood, F. Isothermal P, x, y Data for the Argon + Carbon Dioxide System at Six Temperatures from 233.32 to 299.21 K and Pressures up to 14 MPa. *Fluid Phase Equilib.* **2008**, *273*, 38−43.
(67) Lovseth, S. W.; Skaugen, G.; Jacob Stang, H. G.; Jakobsen, J. P.; Wilhelmsen, Ø.; Span, R.; Wegge, R.; Løvseth, S. W.; Skaugen, G.; Stang, H. G. J.; Jakobsen, J. P.; Wilhelmsen, Ø.; Span, R.; Wegge, R. CO_2Mix Project: Experimental Determination of Thermo Physical Properties of CO_2-Rich Mixtures. *Energy Procedia* **2013**, *37*, 2888−2896.
(68) Kaminishi, G. I.; Arai, Y.; Saito, S.; Maeda, S. Vapor-Liquid Equilibria for Binary and Ternary Systems Containing Carbon Dioxide. *J. Chem. Eng. Jpn.* **1968**, *1*, 109−116.
(69) Fredenslund, A.; Sather, G. A. Gas-Liquid Equilibrium of the Oxygen-Carbon Dioxide System. *J. Chem. Eng. Data* **1970**, *15*, 17−22.
(70) Westman, S. F.; Stang, H. G. J.; Løvseth, S. W.; Austegard, A.; Snustad, I.; Ertesvåg, I. S. Vapor-Liquid Equilibrium Data for the Carbon Dioxide and Oxygen (CO_2 + O_2) System at the Temperatures 218, 233, 253, 273, 288 and 298 K and Pressures up to 14 MPa. *Fluid Phase Equilib.* **2016**, *421*, 67−87.
(71) Christiansen, L. J.; Fredenslund, A.; Gardner, N. Gas-Liquid Equilibria of the CO_2-CO and CO_2-CH_4-CO Systems. In *Advances in Cyrogenic Engineering*, 1995; Vol. *19*, pp 309 −319, DOI: 10.1007/978-1-4613-9847-9_38.
(72) Chapoy, A.; Ahmadi, P.; De Oliveira Cavalcanti Filho, V.; Jadhawar, P. Vapour-Liquid Equilibrium Data for the Carbon Dioxide (CO_2) + Carbon Monoxide (CO) System. *J. Chem. Thermodyn.* **2020**, *150*, No. 106180.
(73) Coquelet, C.; Valtz, A.; Arpentinier, P. Thermodynamic Study of Binary and Ternary Systems Containing CO_2+impurities in the Context of CO_2 Transportation. *Fluid Phase Equilib.* **2014**, *382*, 205−211.
(74) Tsang, C.; Streett, W. B. Phase Equilibria in the H_2/CO_2 System at Temperatures from 200 to 290 K and Pressures to 172 MPa. *Chem. Eng. Sci.* **1981**, *36*, 993−1000.
(75) Clark, A. M.; Din, F.; Robb, J. The Liquid-Vapour Equilibrium of the Binary System Argon/Oxygen. *Proc. R. Soc. London, Ser. A* **1954**, *221*, 517−534.
(76) Bourbo, V. P.; Ischkin, I. Untersuchungen Über Das Gleichgewicht von Flüssigkeit Und Dampf Des Systems Argon-Sauerstoff. Vapor-Liquid Equilibrium in the System Argon-Oxygen. *Physica* **1936**, *3*, 1067−1081.
(77) Pool, A. H.; Saville, G.; Herrington, T. M.; Shields, B. D. C.; Staveley, L. A. K. Some Excess Thermodynamic Functions for the Liquid Systems Argon+Oxygen, Argon+Nitrogen, Nitrogen+ Oxygen, Nitrogen+Carbon Monoxide, and Argon+ Carbon Monoxide. *Trans. Faraday Soc.* **1962**, *58*, 1692−1704.
(78) Sprow, F. B.; Prausnitz, J. M. Vapor-Liquid Equilibria for Five Cryogenic Mixtures. *AIChE J.* **1966**, *12*, 780−784.
(79) Duncan, A. G.; Staveley, L. A. K. Thermodynamic Functions for the Liquid Systems Argon + Carbon Monoxide, Oxygen + Nitrogen, and Carbon Monoxide + Nitrogen. *Trans. Faraday Soc.* **1966**, *62*, 548−552.

Downloaded from pubs.acs.org/jceaax/article-pdf/68/6/1376/9199119/je3c00131.pdf by guest on 30 September 2026

(80) Zenner, G. H.; Dana, L. I. Liquid−Vapor Equilibrium Compositions of Carbon Dioxide−Oxygen−Nitrogen Mixtures. In *Chemical engineering progress symposium series*, 1963; Vol. *59*, no. 44, pp 36 −41.

(81) Vrabec, J.; Kedia, G. K.; Buchhauser, U.; Meyer-Pittroff, R.; Hasse, H. Thermodynamic Models for Vapor−Liquid Equilibria of Nitrogen+oxygen+carbon Dioxide at Low Temperatures. *Cryogenics* **2009**, *49*, 72−79.

Downloaded from pubs.acs.org/jceaax/article-pdf/68/6/1376/9199119/je3c00131.pdf by guest on 30 September 2026

https://doi.org/10.1021/acs.jced.3c00131
J. Chem. Eng. Data 2023, 68, 1376−1387